Initial stages of MnAs heteroepitaxy and nano-island growth on GaAs(110) and (001) surfaces

Motoi Hirayama[1], Gavin R. Bell[1,2], and Shiro Tsukamoto[1]

[1)] *Anan National College of Technology, 265 Aoki, Minobayashi, Anan, Tokushima 774-0017, Japan*

[2)] *Department of Physics, University of Warwick, Coventry CV4 7AL, UK*

(Dated: 4 June 2011)

We have investigated the initial growth of MnAs layers by step-by-step epitaxy on GaAs(110) and GaAs(001). On both surfaces, MnAs nano-crystals developed as the initial stage of MnAs layer formation. Surprisingly, an ultra-high density ($\sim 1 \times 10^{12}\mathrm{cm}^{-2}$) of the nano-crystals with a height of $\sim$5 nm and a size of $\sim$20 nm appeared on GaAs(110). On different surface orientations, the density and the size of the nano-crystals varies. The behavior of the nano-crystallizations can be explained by symmetry at the surface.

I. INTRODUCTION

Many Mn compounds have great potential as materials for spintronic devices. In particular, MnAs is a prototypical ferromagnetic compound compatible with GaAs epitaxy. MnAs may exhibit half-metallicity under some conditions, ideal for an electrode for injection spin-polarized current into non-magnetic GaAs. However, experimentally the spin-injection efficiency reaches only about 6% , which is insufficient for a source of spin-current.[1] To inject completely polarized spin-current into semiconductors, fabrication of well-controlled interfaces between a semiconductor and a robust half-metal are needed.

MnAs has several polymorphs with different structural and magnetic characters; ferromagnetic NiAs-type α-MnAs (hexagonal), paramanetic MnP-type β-MnAs (orthorhombic), paramagnetic NiAs-type γ-MnAs (hexagonal), and ferromagnetic zinc-blende MnAs (cubic).[2] Cubic MnAs have been predicted to be half-metallic by theoretical investigations[3], and the cubic polymorph can be grown in strained nano-island form on GaAs(001) by molecular beam expitaxy (MBE).[4] MnAs thin-films have been grown on various orientations of GaAs surfaces in past studies. The well-aligned interfacial structures of the hexagonal MnAs have been realized on GaAs(001),[5] (111)B,[6] and (110)[7] surfaces. In particular, a GaAs(110) surface has surprisingly good epitaxial match with hexagonal MnAs, with crystallographic relationship GaAs[$1\bar{1}0$]||MnAs[$11\bar{2}0$] and GaAs[001]||MnAs[0001] for the (110) surface.[7] Strong ferromagnetism of the MnAs films is maintained even at very low film thickness.[8]

For spin transport applications, interfacial design depends crucially on the initial growth and epitaxy characteristics. At the initial growth of the MnAs on GaAs surface, formations of nano-crystals with high-density have been widely reported rather than layer-by-layer growth. Nano-crystals of hexagonal MnAs have been formed on the lattice mismatched system with GaAs(001)[9] and (111)B[10] surfaces. The cubic MnAs on GaAs(001) also has high mismatch with epitaxial strain possibly stabilising the polymorph in nano-island form.[4] However, the initial stages of the MnAs growth on GaAs(110) surface have not been systematically investigated. An additional advantage of this growth orientation may also be increased spin lifetime in (110) oriented quantum wells compared to (001).[11] In addition, anisotropic and strongly-localized surface states at GaAs(110) surface give rise to a strong magnetic coupling between Mn atoms, as predicted by a recent theoretical study.[12] Important targets are to clarify the growth process at the interface and to realize strong magnetic coupling.

This paper reports the initial epitaxial growth of MnAs on GaAs(110) and (001) surface. Comparing the two surface orientations we clarify differences of the MnAs growth. Moreover, we present tentative conclusions on the formation mechanisms of the MnAs nano-crystals.

II. EXPERIMENTAL PROCEDURES

Two substrates with GaAs(110) and GaAs(001) surfaces were prepared in standard conditions. Buffer growth on both substrates were performed at 550°C after removing the oxide layers. Starting reconstructions at (110) and (001) surfaces at 350°C were (1×1) and $c(4 \times 4)$, respectively. Step-by-step MBE growth of MnAs was then performed on these surfaces: this is conventional MBE with growth interrupts to perform STM measurements. The substrate temperature was fixed at 350°C. The ratio of As_4/Mn was set to be about 67 and the growth rate was 1.0 ML per 10 seconds. We define the growth rate of MnAs from Mn amounts in the case of MnSb. Because the crystal orientation of MnAs is different on GaAs(001) and (110) we define growth rates by the Mn arrival rate, referencing to the (0001) orientation where 1 ML has thickness $c/2$.[13]

In the initial stage of the MnAs growth, until 3.0 ML total thickness, we irradiated Mn flux for 5 seconds, setting the growth increment to 0.5 ML. These increments were larger subsequently (they are given in Figs. 2 and 3) and the thickness of the MnAs layer finally reached 30 ML in total. We estimate a maximum experimental error of 0.1 ML (1 second) in manual operations of the Mn shutter. After each growth step, surface observations were made using a scanning tunneling microscope (STM) at 200°C without breaking the ultra-high vacuum environment.

III. EXPERIMENTAL RESULTS

We succeeded to observe 3-types nano-crystals on GaAs(110) surface. Circular dots were appeared at 3.0 ML growth, as shown in Fig. 1(a). Increasing the MnAs amount, we got tile-like features on an STM image shown in Fig. 1(b). Top of the tiles have atomically-flat surface, but thickness of the tiles is not atomically-thin. Finally, block crystallites were observed, and seem to have facets like as 3-fold symmetry, as shown in Fig.1(c).

Figure 2 shows STM images of the MnAs layer formed on the GaAs(110) surface by

step-by-step epitaxy. At the initial stage of the MnAs growth, we confirmed that MnAs nano-crystals form on a GaAs(110) buffer layer, not a layer-by-layer growth structure. In fact, MnAs nano-crystals nucleate on the surface with very high density and their size gradually increase as MnAs growth proceeds. After 6.0 ML growth, flat two-dimensional (2D) tiles with approximate square symmetry and circular dots of MnAs were observed to co-exist meaning that the crystallization mode of MnAs changes at around 6.0 ML. Beyond 10 ML growth, the tile-like structure extends parallel to the surface. After a total of 20 ML, the MnAs layer begins to coalesce and crystallize into large granular structures. The size of these grains continuously increases and finally reaches a lateral width of over 200 nm. The grain tops show possible facets with 3-fold symmetry in-plane. These results show that the growth mode changes from 3D nanoparticles to 2D tile-like growth, finally to 3D granular-like growth beyond 20 ML thickness.

On the other hand, the density of the nano-clusters formed on the GaAs(001) surface is an order of magnitude lower than that on the GaAs(110) surface, as shown in Fig. 3. At the initial stage of the MnAs growth on the GaAs(001) surface, the size of the MnAs nano-crystals does not only enlarge, but the density also increases with respect to the MnAs growth. Beyond 6.0 ML MnAs coverage, the nano-crystals coalesce and the density stops growing, and finally large epitaxial crystallites are formed. The nano-crystals readily align in the $\langle 110 \rangle$-direction. The tile-like 2D growth shown on the GaAs(110) surface does not appear on GaAs(001) surface.

To attempt a quantitative analysis of the MnAs growth we first focus on the densities of the nano-crystals. Figure 4(a) shows the changes of the cluster density with respect to the amount of the MnAs layer. In the (110) case we do not distinguish between square tiles and isotropic islands. We regard the maximum error of the number of the nano-crystals as 10 % caused by mainly cluster counting. At the 0.5 ML growth on the GaAs(110) surface, the small nano-crystals with ultra-high density of about $1.0 \times 10^{12}\mathrm{cm}^{-2}$ were formed, as also shown in Fig. 2. The density of the nano-crystals gradually decays with increasing MnAs deposition, caused by the recrystallization or ripening of the nano-crystals.

The behavior of the density of the nano-crystals on the GaAs(001) surface is quite different from that on the GaAs(110) surface. The density on GaAs(001) was saturated at less than $1.0 \times 10^{11}\mathrm{cm}^{-2}$ until the growth amout of 1.0 ML. This value on GaAs(001) surface was ten times lower than the maximum value on GaAs(110) surface, and the densities on each

surface were different over the MnAs amout of 20 ML.

Next, we evaluated the height of the nano-crystals on each surface, as shown in Fig. 4(b). Average heights were measured by ten line-profiles of the STM images in Figs. 2 and 3. On the GaAs(110) surface, the average heights had an extremum value around the MnAs amount of 6.0 ML, from which the MnAs began to recrystallize, discussed above. In other words, the highest nano-crystals around the MnAs amount of 6.0 ML had the most unstable height, and therefore the recrystallizations were easy to proceed. On the other hand, the height on GaAs(001) surface had no extremum in contrast to on GaAs(110) surface, and gradually increased up to more than 15 nm at the MnAs amount of 30 ML. The nano-crystals continued to keep the 3D growth with combinations of the nano-crystals.

Moreover, we also measured the average widths of the nano-crystals, as shown in Fig. 5. The width on the GaAs(110) surface had an extremum value around the MnAs amount of 6.0 ML as well as the average height in Fig. 4(b). In the case on the GaAs(001) surface, the width monotonically increased without any extremum value. No significant geometrical anisotropy of the nano-crystals was observed on both surfaces from either the topological images in Figs. 2 and 3 or the average widths in Fig. 5.

IV. DISCUSSION

We qualitatively consider the onset of the nano-crystallization of the MnAs on the (110) and (001) surfaces in the light of three factors: the formation of reconstructed alloy surfaces, the migration potential of metal adatoms on the GaAs substrate, and the symmetry and epitaxial strain of bulk-like epitaxial MnAs on the two surfaces. In the first place, Mn-adsorbed surfaces have quite different structures between the two GaAs crystal faces. On the GaAs(110) surface, Mn atoms are not strongly bonded in the GaAs matrix at low substrate temperature[14], with isolated Mn atoms physisorbed on the surface, as shown in Fig. 6(a). Conversely, on GaAs(001) Mn atoms form a (2 $\times$ 2) reconstruction at a Mn coverage of 0.25 ML in As-rich conditions[15], as shown schematically in Fig. 6(b). Stable (2 $\times$ 2) structures have been proposed by density functional theory (DFT) calculations[16]. For InAs epitaxial growth on GaAs, alloy formation is also suppressed on the non-polar (110) surface compared to the polar (001) and (111) surfaces[17]. This evidence leads us to expect a lower tendency for Mn to incorporate as a surface alloy on the GaAs(110) surface.

The migration potential for metal adatoms also differs on (110) and (001) surfaces. The energy barriers for Ga adatom migration on GaAs(110) are rather low and anisotropic[18], while Ga on GaAs(001)-c(4×4) has numerous stable adsorption sites due to the high density of anion dangling bonds[19]. It is reasonable to suppose that Mn should also initially experience a lower migration potential on the GaAs(110) surface in our experiments.

Finally, the improved symmetry match[5,7] between MnAs and GaAs(110) compared to GaAs(001) will affect the development of epitaxial morphology. Lower epitaxial symmetry matching necessitates the formation of more misfit-dislocation-like structures in epitaxial nano-islands. This limits the build-up of epitaxial strain compared to the case where a good symmetry match allows fully epitaxial islands to develop. The rapid relaxation of strain in growth on GaAs(001) is consistent with studies of MnSb epitaxy on GaAs,[20] where strain is fully relaxed within the first few ML-equivalent of growth and a high density of misfit dislocations is observed. Furthermore, epitaxial strain can be reduced by surface alloy formation. Given these considerations, it is plausible that epitaxial strain has a stronger effect in the case of GaAs (110) than (001).

MnAs nano-island growth on GaAs(001) is quite simple: the number density remains roughly constant after rapid nucleation (Fig. 4a) and the island size increases monotonically (Fig. 4b and Fig. 5). There are no obvious effects of epitaxial strain on the size distribution, consistent with efficient strain relaxation in the early stages of growth. The lower migration potential of the (110) surface would, at first glance, favour the formation of a lower density of larger islands, since arriving Mn atoms can sample a larger region of the surface to find a stable adsorption site. However, this is the opposite of what is observed (Fig. 4a).

A more complicated picture arises when epitaxial strain and alloy formation are accounted for. Assuming that the MnAs islands on GaAs(110) are more highly strained at the earliest stages of growth, we suggest that strain energy prevents island growth beyond a certain size, i.e. further adatom attachment becomes energetically unfavourable. Such an effect is well known for InAs-GaAs growth, for example.[17] The instability caused by strain allows Mn atoms to detach from nano-islands and join other islands which have developed misfit dislocations. This accounts for the observed ripening of the islands on GaAs(110), whereby the number density falls as the size increases. The rate-limiting step for stable island growth on (110) is thus assumed to be dislocation nucleation, in contrast to (001). The presence of different MnAs island shapes (tiles and dots) on GaAs(110) as well as the unusual behaviour

of the island heights (Fig. 4b) are consistent with a strain-induced morphological change in maturing islands.

We stress that the atomistic mechanisms of the nano-crystal formation are still unknown. Further experimental and theoretical investigations are needed, for example by true in situ STM during molecular beam epitaxy[21,22] and DFT calculations respectively. The latter are limited in the number of atoms which can be considered, a serious problem for complex interfaces, but can predict atomic arrangements, migration potentials and local electronic structures. Recently, hybrid DFT methods have been developed.[23] We expect the formation mechanisms of the nano-crystals can be clarified by such approach, which is able to consider much larger scale regions in atomistic models. Given more elementary understanding of the growth mechanisms of these nano-crystals it may, for example, be possible to control the growth to favour a monodisperse size distribution. Control of the heteroepitaxial growth mechanism should lead to improved interface formation and nanostructure arrays with tailored properties for spin devices.

V. CONCLUSION

We have investigated the initial stage of the MnAs growth on the GaAs(110) surface and the GaAs(001) surface. On both surfaces, the nano-crystals of the MnAs are formed. Surprisingly, an ultra-high density of nano-crystals is formed on the GaAs(110) surface, although familiar growth occurs on the GaAs(001) surface. The difference of the formation processes of the nano-crystals can be explained by the symmetries at the interface. Futher studies of the MnAs nano-crystals and ultra-thin films may reveal physical properties optimisable for applications in spintronic devices, magnetic energy storage and magneto-optical systems.

ACKNOWLEDGMENTS

This research was partially supported by Japan Science and Technology Agency (JST).

REFERENCES

[1]M. Ramsteiner, H. Y. Hao, A. Kawaharazuka, H. J. Zhu, M. Kästner, R. Hey, L. Däweritz, H. T. Grahn, and K. H. Ploog, Phys. Rev. B **66**, 081304 (2002).

[2]K. Kubo, Y. Kato, K. Kanai, J. Ohta, H. Fujioka, and M. Oshima, Journal of Crystal Growth **310**, 4535 (2008).

[3]S. Sanvito and N. A. Hill, Phys. Rev. B **62**, 15553 (2000).

[4]K. Ono, J. Okabayashi, M. Mizuguchi, M. Oshima, A. Fujimori, and H. Akinaga, Journal of Applied Physics **91**, 8088 (2002).

[5]A. Trampert, F. Schippan, L. Däweritz, and K. H. Ploog, Applied Physics Letters **78**, 2461 (2001).

[6]N. Mattoso, M. Eddrief, J. Varalda, A. Ouerghi, D. Demaille, V. H. Etgens, and Y. Garreau, Phys. Rev. B **70**, 115324 (2004).

[7]L. Däweritz, D. Kolovos-Vellianitis, A. Trampert, C. Herrmann, K.H. Ploog, E. Bauer, A. Locatelli, S. Cherifi, and S. Heun, J. Phys. IV France **132**, 159 (2006).

[8]D. Kolovos-Vellianitis, C. Herrmann, L. Däweritz, and K. H. Ploog, Applied Physics Letters **87**, 092505 (2005).

[9]M. Kästner, F. Schippan, P. Schützendübe, L. Däweritz, and K. Ploog, J. Vac. Sci. Technol. B **18**, 2052 (2000).

[10]V. Garcia, M. Marangolo, M. Eddrief, H. Jaffrès, J.-M. George, and V. H. Etgens, Phys. Rev. B **73**, 035308 (2006).

[11]Y. Ohno, R. Terauchi, T. Adachi, F. Matsukura, and H. Ohno, Phys. Rev. Lett. **83**, 4196 (1999).

[12]M. Hirayama, A. Natori, and J. Nakamura, J. Vac. Sci. Technol. B **27**, 2062 (2009).

[13]S. Hatfield and G. Bell, Surface Science **601**, 5368 (2007).

[14]D. Kitchen, A. Richardella, and A. Yazdani, Journal of Superconductivity **18**, 23 (2005).

[15]S. B. Zhang, L. Zhang, L. Xu, E. G. Wang, X. Liu, J.-F. Jia, and Q.-K. Xue, Phys. Rev. B **69**, 121308 (2004).

[16]S. Yang, L. Zhang, H. Chen, E. Wang, and Z. Zhang, Phys. Rev. B **78**, 075305 (2008).

[17]B. A. Joyce, D. D. Vvedensky, T. S. Jones, M. Itoh, G. R. Bell, and J. G. Belk, J. Cryst. Growth **201/202**, 106 (1999).

[18]A. Ishii, T. Aisaka, J.-W. Oh, M. Yoshita, and H. Akiyama, Appl. Phys. Lett. **83**, 4187 (2003).

[19]T. Ito and K. Shiraishi, Jpn. J. Appl. Phys. **35**, L1016 (1996).

[20]S. A. Hatfield and G. R. Bell, Surf. Sci. **601**, 5368 (2007), S. A. Hatfield, Ph.D. Thesis, University of Warwick (2006).

[21]S. Tsukamoto and N. Koguchi, Journal of Crystal Growth **201-202**, 118 (1999).

[22]S. Tsukamoto, T. Honma, G. R. Bell, A. Ishii, and Y. Arakawa, Small **2**, 386 (2006).

[23]S. Ogata and R. Belkada, Computational Materials Science **30**, 189 (2004).

Figure 1:

(Color online) Topographic STM images and line profiles of (a) 3.0 ML (dots), (b) 10 ML (tiles), and (c) 30 ML (crystallites) MnAs on GaAs(110) surface. The size of all images is set to be 300×300 nm^2.

Figure 2:

(Color online) Topographic STM images of MnAs on GaAs(110) surface. The size of all images is set to be 300×300 nm^2. The differences between the maximum and minimum heights are initially 3.9 nm (0.5 ML) and finally 34.2 nm (30ML). These images include the same in Fig. 1.

Figure 3:

(Color online) Topographic STM images of MnAs on GaAs(001) surface. The size of all images is set to be 300×300 nm^2. The differences between the maximum and minimum heights are initially 1.5 nm (0.5 ML) and finally 39.9 nm (30ML).

Figure 4:

(a) Densities and (b) heights of MnAs nano-crystals grown on GaAs(110) and GaAs(001). Values of errorbar are evaluated from standard deviations of sampling data. But it is too small to denote the errorbars on the densities.

Figure 5:

Widths of MnAs nano-crystals grown on (a) GaAs(110) and (b) GaAs(001). Values of errorbar are evaluated from standard deviations of sampling data.

Figure 6:

(Color online) Atomic arrangements of Mn-adsorbed (a) GaAs(110) and (b) GaAs(001). Green, blue, and red balls are indicate Mn, Ga, and As atoms, respectively.

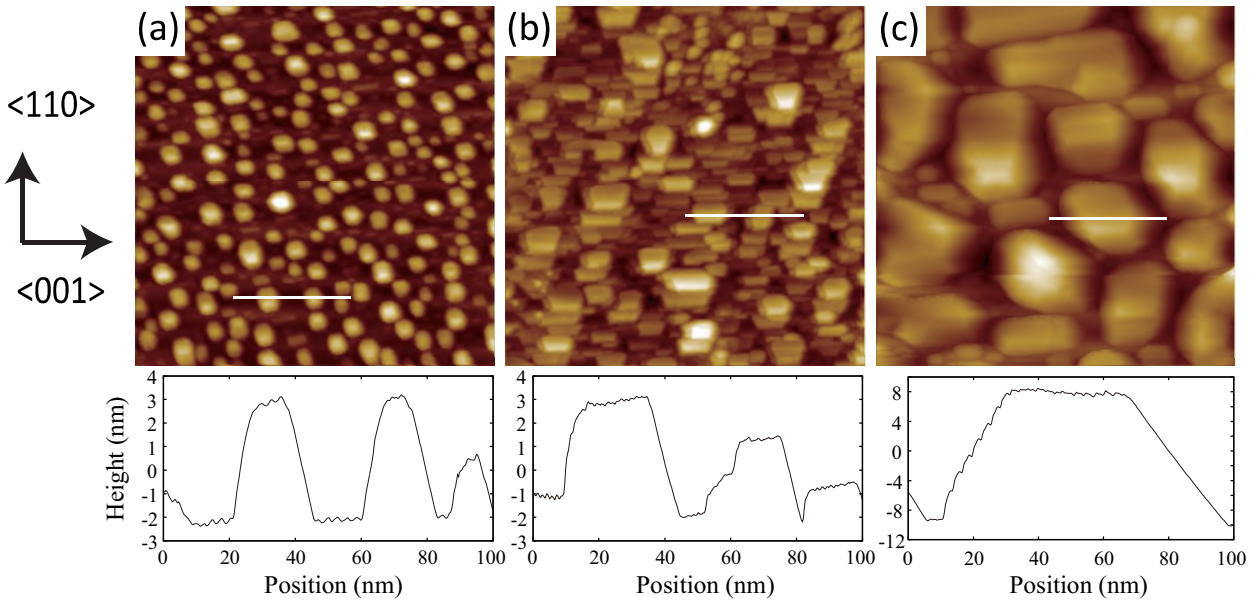

FIG. 1. (Color online) Topographic STM images and line profiles of (a) 3.0 ML (dots), (b) 10 ML (tiles), and (c) 30 ML (crystallites) MnAs on GaAs(110) surface. The size of all images is set to be 300×300 nm^2.

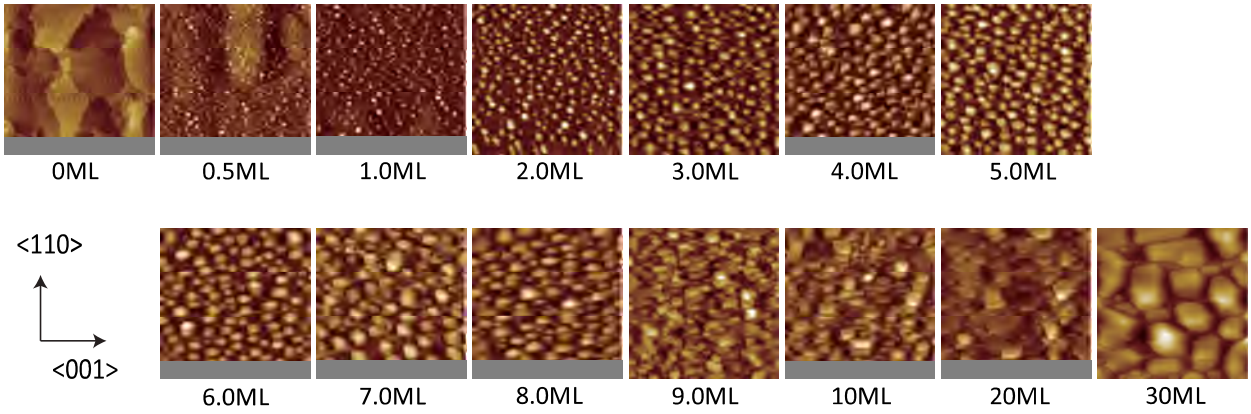

FIG. 2. (Color online) Topographic STM images of MnAs on GaAs(110) surface. The size of all images is set to be 300×300 nm^2. The differences between the maximum and minimum heights are initially 3.9 nm (0.5 ML) and finally 34.2 nm (30ML). These images include the same in Fig. 1.

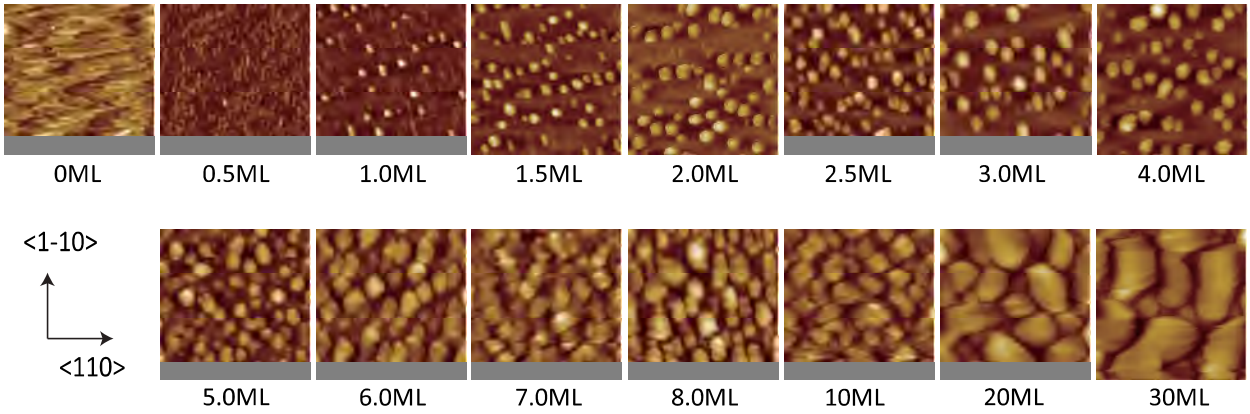

FIG. 3. (Color online) Topographic STM images of MnAs on GaAs(001) surface. The size of all images is set to be 300×300 nm^2. The differences between the maximum and minimum heights are initially 1.5 nm (0.5 ML) and finally 39.9 nm (30ML).

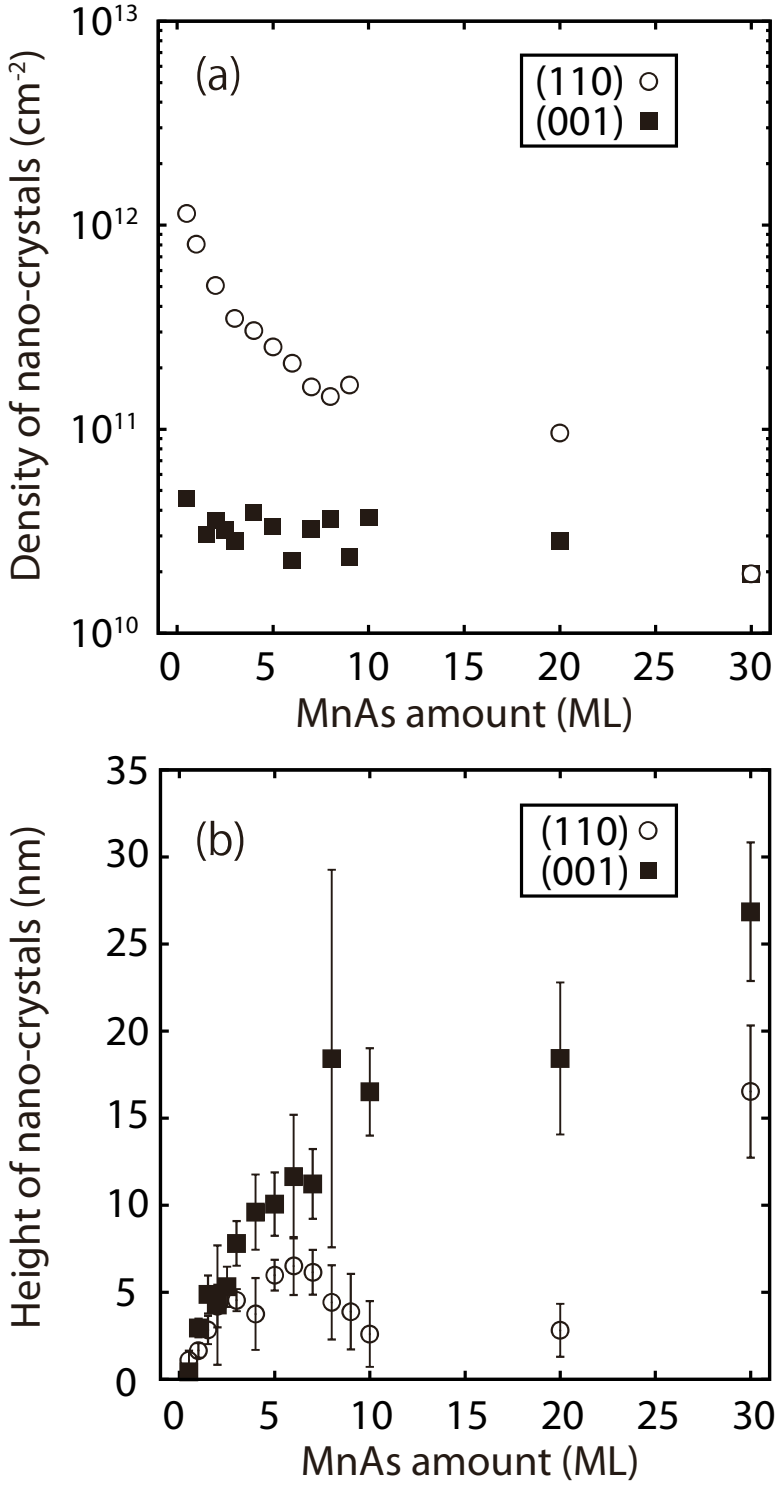

FIG. 4. (a) Densities and (b) heights of MnAs nano-crystals grown on GaAs(110) and GaAs(001). Values of errorbar are evaluated from standard deviations of sampling data. But it is too small to denote the errorbars on the densities.

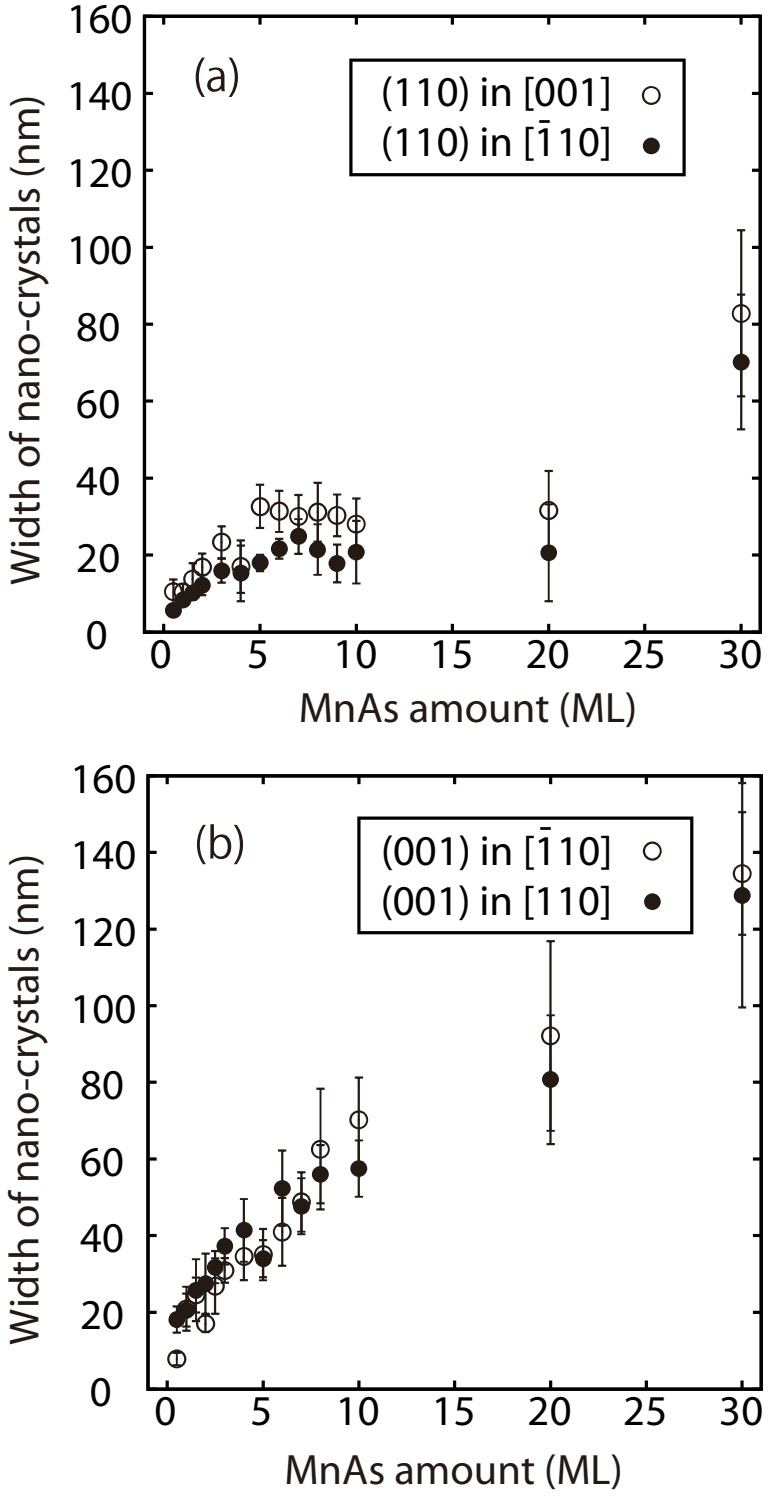

FIG. 5. Widths of MnAs nano-crystals grown on (a) GaAs(110) and (b) GaAs(001). Values of errorbar are evaluated from standard deviations of sampling data.

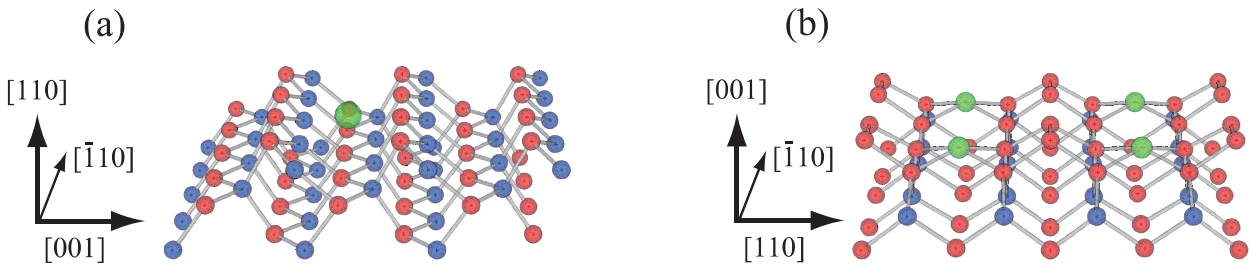

FIG. 6. (Color online) Atomic arrangements of Mn-adsorbed (a) GaAs(110) and (b) GaAs(001). Green, blue, and red balls are indicate Mn, Ga, and As atoms, respectively.